Mutation Research 712 (2011) 33–39

Contents lists available at ScienceDirect

Mutation Research/Fundamental and Molecular Mechanisms of Mutagenesis

journal homepage: www.elsevier.com/locate/molmut
Community address: www.elsevier.com/locate/mutres

Sequence and structural characterization of *tbnat* gene in isoniazid-resistant *Mycobacterium tuberculosis*: Identification of new mutations

Millene Borges Coelho[a,1], Elis Regina Dalla Costa[b,*,1], Sidra Ezídio Gonçalves Vasconcellos[c,1], Natali Linck[a], Ricardo Martins Ramos[a], Hermes Luís Neubauer de Amorim[a,1], Philip Noel Suffys[c], Adalberto Rezende Santos[c], Pedro Eduardo Almeida da Silva[d], Daniela Fernandes Ramos[d], Márcia Susana Nunes Silva[a,b], Maria Lucia Rosa Rossetti[a,b,1]

[a] *Post-Graduation Program in Applied Genetics and Toxicology Program, Lutheran University of Brazil (PPGGTA/ULBRA), Canoas, RS, Brazil*
[b] *Centers for Scientific and Technologic Development, State Foundation for Production and Research in Health (CDCT/FEPPS), Porto Alegre, RS, Brazil*
[c] *Laboratory of Molecular Biology Applied to Mycobacteria, Oswaldo Cruz Institute (IOC/FIOCRUZ), Rio de Janeiro, RJ, Brazil*
[d] *Laboratory of Mycobacteria, Medicine Faculty, Federal University of Rio Grande (FURG), Rio Grande, RS, Brazil*

ARTICLE INFO

Article history:
Received 10 January 2011
Received in revised form 30 March 2011
Accepted 31 March 2011
Available online 14 April 2011

Keywords:
Mycobacterium tuberculosis
Drug resistance
Mutation
tbnat Polymorphism
Structure–function
Molecular modeling

ABSTRACT

The present study was carried out to investigate the presence of polymorphism in the *N*-acetyltransferase gene of 41 clinical isolates of *Mycobacterium tuberculosis,* that were resistant to isoniazid (INH) with no mutations in the hot spots of the genes previously described to be involved in INH resistance (*kat*G, *inh*A and *ahp*C). We observed single nucleotide polymorphisms (SNPs) in ten of these, including the G619A SNP in five isolates and an additional four so far un-described mutations in another five isolates. Among the latter SNPs, two were synonymous (C276T, $n = 1$ and C375G, $n = 3$), while two more non-synonymous SNPs were composed of C373A (Leu→Met) and T503G (Met→Arg) were observed in respectively one and two isolates. Molecular modeling and structural analysis based in a constructed full length 3D models of wild type TBNAT (TBNAT_H37Rv) and the isoforms (TBNAT_L125M and TBNAT_M168R) were also performed. The refined models show that, just as observed in human NATs, the carboxyl terminus extends deep within the folded enzyme, into close proximity to the buried catalytic triad. Analysis of *tbnat* that present non-synonymous mutations indicates that both substitutions are plausible to affect enzyme specificity or acetyl-CoA binding capacity. The results contribute to a better understanding of structure–function relationships of NATs. However, further investigation including INH-sensitive strains as a control group is needed to get better understanding of the possible role of these new mutations on tuberculosis control.

1. Introduction

Isoniazid (INH) is one of the main drugs used in tuberculosis treatment [1,2], and the resistance to this drug has been associated to mutations in several genes including at least *kat*G, *inh*A and *ahp*C [3–6], however, 20–30% of the INH resistant isolates do not show mutation in these genes, suggesting the involvement of other genes or mechanisms, examples being the *tbnat* gene [7–10] or efflux pumps [11].

Arylamine *N*-acetyltransferases (NAT) belong to a family of cytosolic enzymes found in eukaryotes and prokaryotes and catalyze the *N*-acetylation of arylamine and hidrazines by transferring an acetyl group to the terminal nitrogen group of the substrate, using acetyl coenzyme A as a cofactor. These enzymes are also able to catalyze the transfer of an acetyl group to the oxygen of arylhydroxylamines [12–14]. It has been already described that NAT performing catalysis via a bi-bi ping pong mechanism, transferring an acetyl group from the acetyl-CoA (donor) to a NAT enzyme, forming a acetylated intermediate, followed by a second transfer to the substrate [14–16]. Being mostly studied in eukaryotes, data show that prokaryotic NAT acetylates INH [14,17,18]. Also, it has been demonstrated that NAT is expressed endogenously in *M. smegmatis* and the NAT proteins from Mycobacteria can acetylate and inactivate *in vitro* isoniazid [18], suggesting that this enzyme may be involved in INH susceptibility [19]. Also, it has been proposed that there is a competition between the catalase-peroxidase (CP)

* Corresponding author at: Centro de Desenvolvimento Científico e Tecnológico (CDCT); Fundação Estadual de Produção e Pesquisa em Saúde (FEPPS), Av Ipiranga 5400, 3° andar, CEP 90610 000, Porto Alegre, Rio Grande do Sul, Brazil.
Tel.: +55 51 3352 0336; fax: +55 51 3352 0336.
E-mail address: erdallacosta@yahoo.com.br (E.R.D. Costa).
[1] Equal contributors.

0027-5107/$ – see front matter © 2011 Elsevier B.V. All rights reserved.
doi:10.1016/j.mrfmmm.2011.03.017

protein (encoded by *kat*G) and the NAT enzyme for INH [14]. Activation of INH in *Mycobacterium tuberculosis* by catalase–peroxidase involves oxidation of the hydrazine moiety, which cannot occur when INH is *N*-acetylated [12]. We analyzed the entire *tbnat* gene from INH-resistant clinical isolates with no mutations in *kat*G, *inh*A and *ahp*C genes. The implications of the observed mutations in *tbnat* function are suggested with basis on the analysis of structural models obtained by computational techniques.

2. Materials and methods

2.1. M. tuberculosis strains selection

A collection of 265 *M. tuberculosis* isolates considered INH resistant, both by the proportion and by determining Minimum Inhibitory Concentration (MIC) method was selected and screened for the presence of mutations in hot spots of *kat*G, *inh*A and *ahp*C genes, known to be involved in INH resistance and this led to the characterization of 41 isolates with WT alleles in these genes. These strains were from patients diagnosed with TB between September 2003 to December 2004 and were identified to the species level by analysis of the morphologic and biochemical characteristics [20].

This work was approved by Ethics Committee of Lutheran University in Brazil (CEP-ULBRA 2007-353H).

2.2. Proportion method

All 265 strains and the reference strain were tested for susceptibility with the proportion method on Lowenstein–Jensen (LJ) medium [21] in the absence and presence of INH (0.2 μg/mL). Reference strain *M. tuberculosis* H37Rv ATCC 27294 was used as INH susceptible strain control.

2.3. Minimum inhibitory concentration (MIC) determination

The test was performed as described by [22] to all the strains. The INH (Sigma, St. Louis, MO, USA) stock solution was prepared at concentration of 10 mg/mL in sterile distilled water. Serial two-fold dilutions of INH in 100 μL of Middlebrook 7H9 broth medium (Difco, Detroit, MI, USA) containing glycerol enriched with 10% oleic acid–albumin–dextrose–catalase (OADC) and Bacto Casitone (Difco) were prepared directly in 96-well flat-bottom microplates (Corning Costar, Cambridge, MA, USA) with final INH concentrations from 16 to 0.2 μg/mL (200 μL total volume). The inoculum was prepared from fresh LJ medium in Middlebrook 7H9 broth medium adjusted to a McFarland symbol 1 and then further diluted 1:20. A 100 μL aliquot of this dilution was added into each well. The microplates were covered, sealed in plastic bags, and incubated at 37 °C in the normal atmosphere. After 7 days of incubation, 30 μL of resazurin solution was added to each well, incubated overnight at 37 °C for 48 h and evaluated for color change. Resazurin sodium salt powder (Acros Organic N.V.) prepared at 0.01% (wt/vol) in distilled water was used as a general indicator of cellular growth and viability. A change from blue to pink indicates reduction of resazurin and therefore bacterial growth. The MIC was defined as the lowest drug concentration that presented no color change. The cut off value for resistance was ≥0.2 μg/mL according to [22]. Growth controls containing no INH and sterility controls without *M. tuberculosis* were included in each MIC testing.

2.4. Nucleic acid extraction

M. tuberculosis chromosomal DNA was extracted from culture recovered strains using the CTAB method as described by [23].

2.5. PCR amplification and sequence analysis

The following hot spot genes were amplified by using genomic DNA as template for PCR amplification with the following primers katG 1: 5′ CAT GAA CGA CGT CGA AAC AG 3′, katG 2: 5′ CGA GGA AAC TGT TGT CCC AT 3′; ahpC 1: 5′ GCC TGG GTG TTC GTC ACT GGT 3′, ahpC 2: 5′ CGC AAC GTC GAC TGG CTC ATA 3′; inhA (ORF) 1: 5′ GAA CTC GAC GTG CAA AAC 3′, inhA (ORF) 2: 5′ CAT CGA AGC ATA CGA ATA 3′; inhA (reg) 1: 5′ CCT CGC TGC CCA GAA AGG GA 3′, inhA (reg) 2: 5′ ATC CCC CGG TTT CCT CCG GT 3′, as described by [9], yielding fragments of 232 bp, 359 bp, 206 bp and 248 bp, as described by [24], respectively. Amplification products were analyzed by electrophoresis in 1.5% agarose gels purified with MicroSpin S-300 HR Columns (Amersham Biosciences, Piscataway, NJ, USA) and sequenced by using the Big Dye Terminator Cycle Sequencing Kit with AmpliTaq DNA polymerase (Applied Biosystems, Foster City, CA, USA) in the ABI Prism 3100 DNA Sequencer (Applied Biosystems).

Genomic DNA was used as template for PCR amplification of the *tbnat* gene with specific primers binding 69 bp upstream and 110 bp downstream from the *tbnat* gene as follows: *tbnat* 1 forward: 5′ ATC GGT GCG ACA TAG TTG G 3′ and *tbnat* 4 reverse: 5′ GCC TTC TGC TCA AAG TTG CT 3′. The PCR was performed on a GeneAmp PCR System 9700 thermocycler (Applied Biosystems) in a final volume of 50 μl containing 40 pmol of each primer, 2.5 mM MgCl2, 0.2 mM dNTPs, 1U *Taq* DNA polymerase (Invitrogen, Brazil), PCR-buffer (10 mM Tris–HCl, 1.5 mM MgCl2, 50 mM KCl, pH 8.3) (Invitrogen, Brazil), 10% glycerol, and 10 ng of target DNA as follows: 95 °C for 5 min, 65 °C for 1 min and 30 s, 72 °C for 1 min, for 40 cycles and a final cycle of 72 °C for 4 min. Amplification products were analyzed by electrophoresis in 1.0% agarose gels, purified with QIAquick PCR Purification kit (QIAGEN) and the 1069 bp *tbnat* fragment was also sequenced using internal primers (*tbnat* 2 reverse internal: 5′ GTC CTC GAG CCG ATA AGG GTT 3′ and *tbnat* 3 forward internal: 5′ CAC CGA CCT CAC CGC TTC 3′). The design of primers used for PCR amplification and sequence was based on the published genome sequence of *M. tuberculosis* H37Rv (6) with aid of PRIMER3 Program. Sequencing was performed at the Oswaldo Cruz Foundation (PDTIS DNA Sequencing Platform/FIOCRUZ, Rio de Janeiro – RJ, http://www.dbbm.fiocruz.br/PDTIS_Genomica/) in accordance with described by [25] and the results were analyzed with MegAling (DNASTAR Inc., Madison, Wis.) and SeqScape v 2.6 (Applied Biosystems) and the H37Rv sequence (Rv3566c) was used as reference.

2.6. Spoligotyping

Spoligotyping was performed as described by [26]. The found spoligopatterns were compared to those in the international database of SpolDB4 (http://www.pasteur-guadeloupe.fr: 8081/SITVITDemo/).

2.7. Molecular modeling

Structural models for TBNAT isoforms (H37Rv, M168R and L125 M) were generated by homology modeling using the MODELLER 9v7 software [27,28] (http://salilab.org/modeller/). The first step was to search for homologous proteins of NAT from *M. tuberculosis* H37Rv (TBNAT, amino-acid sequence access code YP_177989 in the NCBI database) whose experimental structures are available in the Protein Data Bank (PDB). Two structures were chosen as templates, NAT from *Mycobacterium marinum* (MMNAT), PDB ID: 2VFB (2.0 Å resolution, 76% sequence identity), and NAT from *M. smegmatis* (SMNAT), PDB ID: 1W6F (2.1 Å resolution, 61% sequence identity). The sequences of the nonnative isoforms were obtained by the substitution of the specific amino-acids in the FASTA file containing the sequence of the wild type (*tbnat*_ H37Rv) enzyme: leucine (L) at position 125 by an metionine (M) (TBNAT_L125 M) and metionine (M) at position 168 by an arginine (R) (TBNAT_M168R). One hundred models were independently generated for each isoform. Those models that showed the most negative value for the DOPE energy function [29] were chosen for a more detailed analysis.

The lack of resolution for C-terminal segment in available crystal structures of prokaryotic NATs resulted that the corresponding region in the homology models was disordered. Thus, in order to obtain a suitable template to TBNAT structures, an additional stage of refinement was performed by a 10 ns molecular dynamics (MD) simulation of TBNAT H37Rv model. The final structure of MD simulation was utilized as template to generate new models of TBNAT_ H37Rv, TBNAT_L125 M and TBNAT_M168R. The protocol used to perform the MD simulation is described in [30].

3. Results and discussion

3.1. Mutations

The present study was carry out aiming investigate the presence of polymorphism in the *N*-acetyltransferase gene and efflux pumps mechanisms in 41 *M. tuberculosis* INH resistant (INH-R) clinical isolates that did not have mutations in regions of genes previously shown to be involved in INH resistance (*kat*G, *inh*A and *ahp*C) [3–6]. The CDS *tbnat* gene was completely sequenced in all of the isolates and single nucleotide polymorphisms were identified in ten out of forty one isolates tested (Table 1). The already described G619A NAT SNP, responsible by the amino acid change (gly to arg) was observed in 5 isolates (12.2%). This SNP has been already described in literature with a frequency of 619-A SNP in 12% and 20% of a random cohort of clinical isolates [12,13]. In a previous study performed in isolates from Brazil, this SNP was observed in 5.2% of the isolates [25]. The observed difference among the frequencies could be explained because of the number of samples selected, selection criterion or genetic differences among the isolates investigated.

Upon sequence analysis we also observed so far undescribed four new SNPs, two synonymous SNPs, C276T and C375G, and two non-synonymous, T503G and C373A, responsible by changes in the amino acid (Met→Arg) at the codon 168 and (Leu→Met) at the codon 125, respectively. Allele frequencies, calculated from the total of the tested samples (41 isolates) showed the higher incidence of the SNP C375G among the new SNPs identified (0.0073),

Table 1
CDS *nat* gene mutation, its genotyping and MIC, in *kat*G, *inh*A and *ahp*C WT *M. tuberculosis* isolates.

Isolate	aa Change	*nat* SNP	Reference	Effect	Genotyping	MIC
A-6972	G619A SNP (G207R)	GGA/AGA	[12]	Non-synonymous	LAM3 S/convergente	0.125
PA-727	G619A SNP (G207R)	GGA/AGA	[12]	Non-synonymous	T3	16
PA-1114	G619A SNP (G207R)	GGA/AGA	[12]	Non-synonymous	Not described[c]	≤ 0.125
CE-588	G619A SNP (G207R)	GGA/AGA	[12]	Non- synonymous	LAM3 S/convergente	0.2
342/04	G619A SNP (G207R)	GGA/AGA	[12]	Non-synonymous	T1	≤0.25
A-6906	C276T SNP[a] (A92A)	GCC/GCT	In this study	Synonymous	Beijing	≤0.25
A-7390	C373A SNP[b] (L125M)	CTC/ATG	In this study	Non-synonymous	Not described[c]	≤0.25
	C375G SNP[a] (L125L)	CTC/ATG	In this study	Synonymous		
CE-3920	C375G SNP[a] (L125L)	CTC/CTG	In this study	Synonymous	LAM6	1
RS-345	C375G SNP[a] (L125L)	CTC/CTG	In this study	Synonymous	LAM9	0.5
	T503G SNP[b] (M168R)	ATG/AGG	In this study	Non-synonymous		
RS-363	T503G SNP[b] (M168R)	ATG/AGG	In this study	Non-synonymous	T1 (T4-CE1 ancestor?)	0.5

[a] New *M. tuberculosis* nat gene mutations not described yet.
[b] Non-synonymous new *M. tuberculosis* nat gene mutations not described yet.
[c] Not described means that they are not present at the SpolDB4 [41].

followed by SNP T503G (0.0048) and SNPs C276T, C373A (0.0024). Coexistence of new SNPs and the already described G619A was not achieved in any isolate; however, in two isolates the presence of synonymous and non-synonymous SNPs was observed (Table 1).

3.2. General analysis of the TBNAT homology models

Low solubility of recombinant TBNAT has hampered detailed structural crystallographic studies of this enzyme [16]. In order to overcome the lack of 3D information, structural models of wild type TBNAT (TBNAT_H37Rv) and isoforms (TBNAT_L125 M and TBNAT_M168R) sequenced in INH resistant *M. tuberculosis* isolates were obtained by homology modeling.

Two crystal structures were used as templates, the arylamine N-acetyltransferase of *M. smegmatis* (MSNAT) and the arylamine N-acetyltransferase of *M. marinum* (MMNAT). These enzymes were chosen because of the high degree of homology with TBNAT (61%, SMNAT; 76%, MMNAT). *M. marinum* is one of the most closely related organisms to the pathogenic *M. tuberculosis* complex [31,32]. The amino acid sequence of MMNAT enzyme shares 73% of identity and 84% of similarity to TBNAT. In this regard, MMNAT is more similar to the TBNAT enzyme than any other recombinant NAT enzyme expressed to date [14,16]. Also, the MMNAT substrate specificity profile is very similar to that for TBNAT [32]. Regarding to MSNAT template, in addition to the high degree of homology, is known that the NAT enzyme from *M. smegmatis* acetylates isoniazid [18]. In fact, expression of *M. tuberculosis tbnat* gene in *M. smegmatis* leads to an organism with increased resistance to isoniazid [19]. Moreover, MSNAT is the unique NAT enzyme whose experimental structure is available in complex with isoniazid [33].

Table 2 compares the structural parameters of MMNAT and SMNAT, template structures, with the parameters obtained for the wild type and mutant TBNATs. The quality of the templates and of the homology models was evaluated using the programs PROCHECK [34], VERIFY 3D [35] and Errat [36] implemented on SAVES (Stuctural Analysis and Verification Server, http://nihserver.mbi.ucla.edu/SAVES/). The values of the analyzed parameters show the good quality of the homology models.

As expected, the fold of TBNAT_H37Rv model (and isoforms) resembles the general fold observed in mammalian and prokaryotic NATs (Fig. 1). The amino-terminal domain (residues 1–85) consists of five helices (α1–α5). The second domain comprises residues 86–184 and consists of eight β-strands (β2–β9). These two domains connect through the α-helical interdomain (helices α6–α7, residues 185–208), to the third domain (residues 209–283), which has four anti-parallel β-strands (β10–β13) and two helices (α8–α9). The refined TBNAT_H37Rv model shows that, just as observed in human NATs, the carboxyl terminus extends deep within the folded enzyme, into close proximity to the buried catalytic triad. The structural arrangement observed for C-terminal region is noteworthy, since it had not been determined [37], and may be common for other prokaryotic NATs. In this regard, it is believed that C-terminus of prokaryotic NATs may have a role in regulating the binding of acetyl-CoA in the absence of substrate [38].

3.3. Interactions of wild type TBNAT with acetyl-CoA and isoniazid

There are evidences that at least in prokaryotic NATs part of the acetyl-CoA binding site overlaps with the binding site of the acetyl group acceptor (e.g. arylamines and hydrazines). Such evidence comes from comparison between crystallographic structures of MMNAT complexed with acetyl-CoA and MSNAT complexed with INH. In the crystallographic MSNAT-isoniazid complex, the terminal nitrogen atom of the hydrazyl group is positioned at 2.4 Å of the Sγ of the catalytic cysteine residue (Cys70) [33]. Furthermore, the INH hydrazyl group makes one hydrogen bond with the backbone carbonyl group of Thr109 while the aromatic moiety of the drug interacts through hydrophobic contacts with Phe38, Val95, Phe130, and Phe204. Similar to binding of isoniazid observed in MSNAT complex, in the MMNAT-acetyl-CoA complex the terminal sulfhydryl moiety of CoA is positioned 2.8 Å from Sγ of Cys70, in an environment constituted of aromatic residues Phe38, Tyr69, Tyr71, His110, Phe130 and Phe204 [16]. Among the aminoacid residues used by MMNAT for CoA binding, Phe38, Cys70, Phe130 and Phe204 are used by MSNAT to make contacts with isoniazid in the MSNAT-INH complex. In order to estimate the binding forms of the two ligands, the relative coordinates of the acetyl-CoA from MMNAT-acetyl-CoA complex and isoniazid from MSNAT-INH complex were transposed to TBNAT model (Fig. 2).

The location of amino-acid residues that are possibly involved in the binding of CoA and INH to wild-type TBNAT are shown in Fig. 3. The amino acid positions that have undergone punctual substitutions leading to new TBNAT isoforms, observed in isolates of resistant *M. tuberculosis*, are also represented. In the crystallographic complex, MMNAT interacts with acetyl-CoA through the following amino acid residues: Phe38, Tyr69, Tyr71, Cys70, Trp97, His110, Phe130, Gly132, Glu152, Val169, Phe204, Thr209, Ala211, Ser222, His229, and Lys236 [16]. These, thirteen are structurally conserved in TBNAT, except Tyr71, Met209 and Met222, that are substituted by Phe71, Thr209 and Ser222 (Fig. 3). While the substitution Tyr→Phe may be considered conservative, the substitutions at TBNAT domain III, Met→Thr and Met→Ser, are nonconservative. In the MMNAT, the side-chain carbon atoms of Met209 and Met222 are involved in the accommodation of the dimethyloxybutyl moi-

Table 2
Comparative of the quality of template and model structures.

Template or model	Procheck					Verify 3D	Errat
	Core	Allow.	Gener.	Desall.	Overall G-factor[a]		
MMNAT	85.6	12.2	1.3	0.9	−0.1	99.27	97.34
MSNAT	90.4	9.2	0.4	0.0	−0.07	99.64	96.89
TBNAT_H37Rv	89.6	9.6	0.8	0.0	−0.14	91.90	80.45
TBNAT_L125M	87.5	11.7	0.0	0.8	−0.15	92.96	69.00
TBNAT_M168R	90.0	8.8	0.4	0.8	−0.14	91.90	77.98

[a] dihedral G-factor [42].

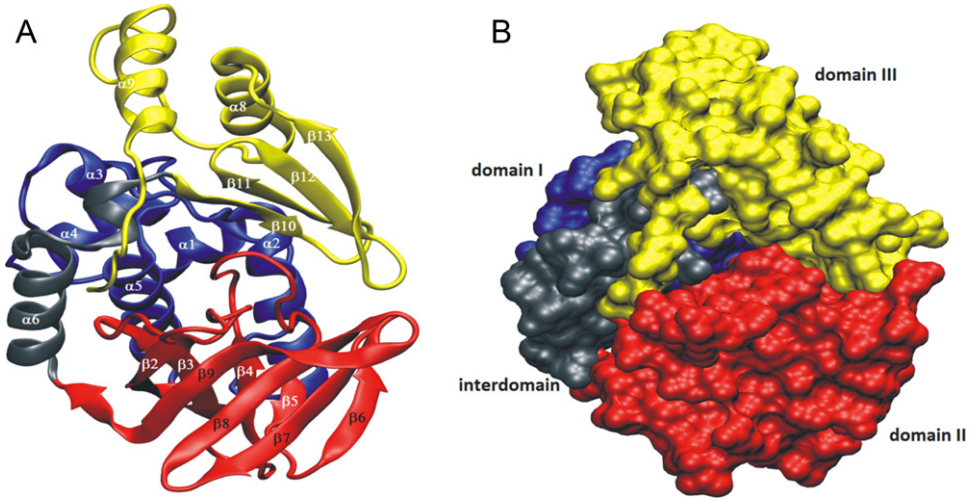

Fig. 1. Schematic representations of the refined TBNAT model. Domain I in red, domain II in blue, interdomain in gray and domain III in yellow. (A) Ribbon trace. (B) Molecular surface. (For interpretation of the references to color in text, the reader is referred to the web version of the article.

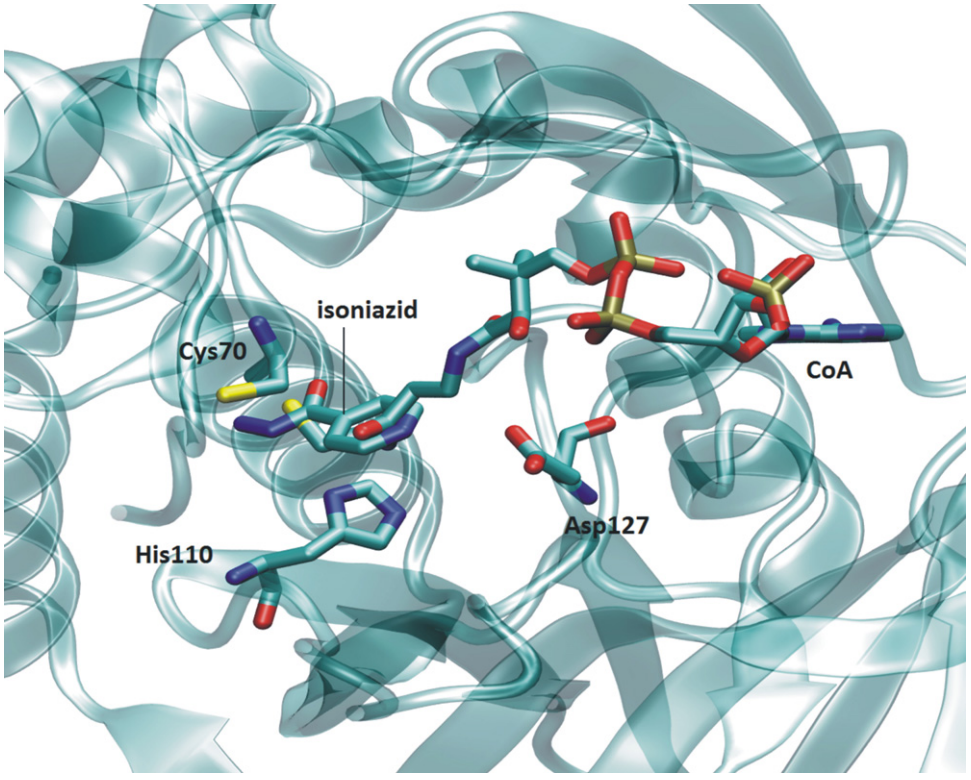

Fig. 2. Comparison of the probable binding modes of CoA and isonizaid to TBNAT. Interaction model based on the binding mode of CoA to MMNAT and isoniazid to MSNAT TBNAT fold is represented in ribbon trace. TBNAT catalytic triad, CoA and isoniazid are represented in licorice.

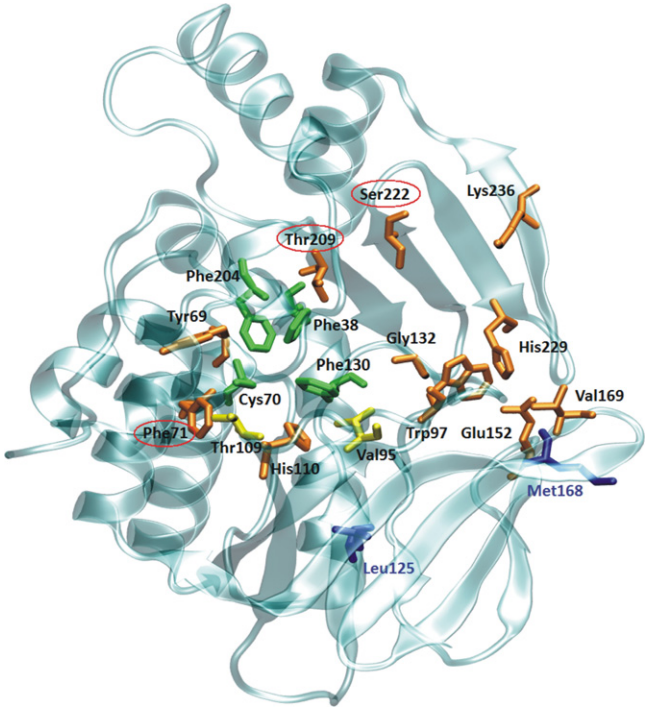

Fig. 3. Amino-acid residues that are possibly involved in the binding of CoA and INH to wild-type TBNAT. Prediction based in the MMNAT-CoA and MSNAT-INH crystallographic complexes. Amino acid residues that interact exclusively with CoA are shown in orange. Amino acid residues that interact exclusively with isoniazid are shown in yellow. Amino acid residues that interact with CoA and isoniazid are shown in green. Except the amino acid residues highlighted by ellipses the others are conserved in MMNAT. Represented in blue are the amino acid positions that have undergone punctual substitutions leading to new TBNAT isoforms (see text). (For interpretation of the references to color in text, the reader is referred to the web version of the article.

ety located at the pyrophosphate end of the pantotheinate arm of CoA [16]. In this context, it has been proposed that the role of interactions between domain III of prokaryotic NATs and CoA is to keep CoA bound to the acetylated enzyme intermediate until a suitable acetyl group acceptor displaces it [16]. Considering that the maintenance of CoA associated to enzyme can act to minimize acetyl-CoA hydrolysis, it is possible that, at least in part, lower catalytic efficiency of wild type TBNAT when compared to MMNAT is due to less efficient interactions of the former with its cofactor. In turn, this effect can be attributed to Met→Thr and Met→Ser substitutions at domain III. This latter hypothesis is in agreement with evidences that support that the third domain has a role in substrate specificity of NAT enzymes [38].

3.4. TBNAT isoforms in resistant M. tuberculosis isolates

Three structural models were generated from the alleles presenting the wild type *tbnat* sequence and from those presenting the non-synonymous mutations C373G (Leu→Met, TBNAT_L125 M isoform) or T503G (Met→Arg, TBNAT_M168R isoform) (Fig. 4).

The TBNAT C373G allele encodes the substitution of Leu125 by Met (TBNAT L125 M). This substitution, involving the exchange of a branched (Leu) by a linear (Met) side-chain, is located on β4 strand. Analysis of TBNAT_L125 M model shows that a probable rearrangement of the enzyme main chain is necessary for the accommodation of the Met side-chain. It is possible that the Leu→Met substitution generates local disturbances affecting the conformation and/or dynamics of residues situated at the bottom of the cleft for substrate and acetyl-CoA binding (e.g. Val95, Trp97, His110), thus influencing the specificity or catalytic activity of the enzyme.

The T503G mutation is responsible for Met168Arg substitution (TBNAT M168R), located at β8 strand, which comprises one of the sheets that bind CoA in MMNAT. Furthermore, the residue at position 168 is adjacent to Val169 and near to Glu152. In MMNAT-CoA complex, the side-chain of Val169 forms hydrophobic interactions with the adenine moiety of CoA while the side-chain carboxyl oxygen of Glu152 interacts through a hydrogen bond with the exocyclic nitrogen atom of the adenine base. Therefore, presuming that the binding capacity of the acetyl-CoA to TBNAT is important for the catalytic activity, the possibility of Met168Arg mutation to affect the enzymatic efficiency must be considered.

In a previous study it was shown that the interaction of TBNAT with isoniazid is low affinity [40]. In another work Fullan e colleagues pointed that, when the substrate is 5-aminosaliclyate, the affinity of TBNAT for acetyl-coenzyme is lower than that of the MMNAT [32]. These results indicate that, unless in the cases of over expression, the role of wild-type *tbnat* as a source of *M. tuberculosis* resistance to isoniazid is questionable. On the other hand, our results clearly show that the substitutions detected in the isoniazid resistant strains are capable to affect the binding capacity of both acetyl-coenzyme and isoniazid and, in turn, influence the affinity and/or the catalytic ability of the mutant enzymes. For instance, with respect to isoniazid, the catalytic efficiency of the highly homologous enzyme MMNAT ($k_{cat}/K_m = 274\ M^{-1}\ s^{-1}$) [32] is about six times larger than the TBNAT ($k_{cat}/K_m = 49\ M^{-1}\ s^{-1}$) [2].

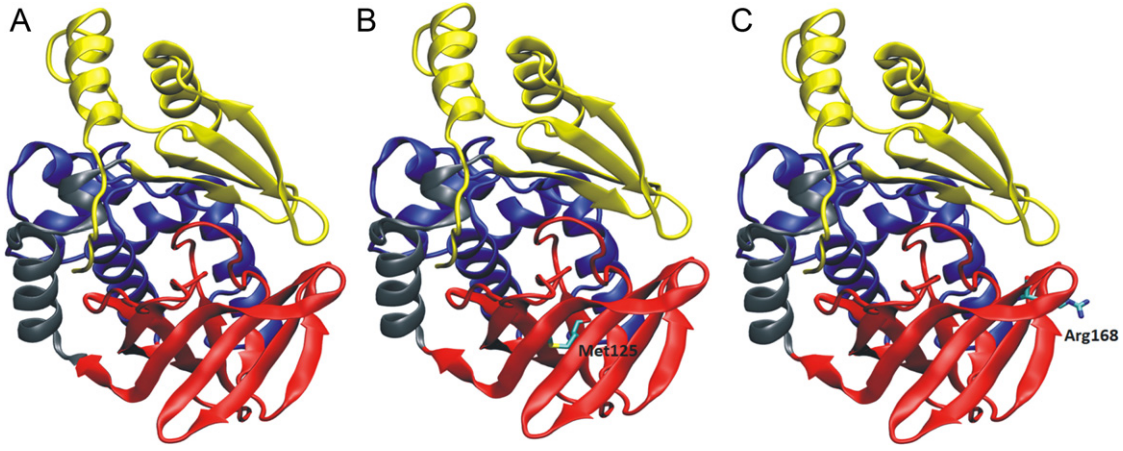

Fig. 4. Ribbon models of wild-type and mutant TBNATs. Wild-type TBNAT (A), TBNAT_L125 M (B) and TBNAT_M168R (C). Domain I in red, domain II in blue, interdomain in gray and domain III in yellow. Substituted residues are shown in licorice representation. (For interpretation of the references to color in text, the reader is referred to the web version of the article.)

If any of the described mutations act in order to increase the catalytic activity, the *tbnat* role in the development of resistance to isoniazid need to be reconsidered as well as new strategies for treating drug-resistant TB should be planned. Clearly, future work should demonstrate whether such substitutions have the ability to increase or decrease the enzyme activity of the mutant forms.

3.5. Spoligotyping

The strain families that could be grouped by SpolDB4 included: LAM (41.5%, $n = 17$), Haarlem (22%, $n = 9$), *T* (12.2%, n = 5), *X* (4.9%, $n = 2$), *U* (2.4%, $n = 1$) and Beijing (4.9%, $n = 2$). Five (12.2%) isolates had an unclassified spoligopattern. In one of these was found the G619A SNP and in other one was found the new SNP L125 M. It was observed 9 different spoligotypes in the 10 mutated strains, meaning that none of the mutated strains belong to a cluster (Table 1). In addition, no association was observed between any SNP and a spoligotype family, including the variant 619-A NAT [$p = 0.87$; OD = 0.85 (0.07–9.76)]. Also, it was not found association between new mutations in *tbnat* gene and a specific spoligopattern ($p = 0.31$; OD = 0.52; 0.11–2.29).

3.6. Minimum inhibitory concentration (MIC) determination

All isolates previously shown to be INH resistant by the proportion method were tested to determine the MIC levels. In 5 of them, the MIC values were ≤0.125 and in two of these appear the G619A SNP. In tree isolates the MIC was ≤0.25 and in all of them appear *tbnat* mutations (Table 1). Most of the isolates showed low MIC values and in only 7 isolates the MIC were ≥2 μg/mL. In the opposite, in studies carried out in INH resistant isolates showing *kat*G mutation, especially at the 315 codon, the MIC levels used to be ≥2 μg/mL, which is considered high INH MIC values [10,39]. Possible relationship between efflux mechanism and low level resistance was not found (data not shown).

4. Summary

A refined full length structural model for wild type TBNAT was proposed and analysis of TBNATs that have suffered non-synonymous mutations indicated that all amino acid substitutions are plausible to affect enzyme specificity or acetyl-CoA binding capacity. Although the binding of isoniazid to TBNAT is a low affinity interaction [40], the possibility of the described mutations affecting the enzyme structure to increase its affinity for drug and thus representing a new source of resistance to *M. tuberculosis* should be considered. Docking and molecular dynamics simulations are in progress to better characterize the effect of mutations on the TBNAT affinity. Finally, the results obtained in this work should contribute to a better understanding of structure-function relationships of NATs as well as for to direct drug design target to resistant tuberculosis.

Conflict of interest statement

The authors declare no conflict of interest.

References

[1] Y. Zhang, A. Telenti, Genetics of drug resistance in Mycobacterium tuberculosis, in: G.F. Hatfull, W.R. Jacobs Jr. (Eds.), Molecular Genetics of Mycobacteria, ASM Press, Washington DC, 2000, pp. 235–253.
[2] G.S. Timmins, V. Deretic, Mechanisms of action of isoniazid, Mol. Microbiol. 62 (2006) 1220–1227.
[3] A. Banerjee, E. Dubnau, A. Quemard, V. Balasubramanian, K.S. Um, T. Wilson, D. Collins, G. Lisle, W.R. Jacobs Jr., inhA, a gene encoding a target for isoniazid and ethionamide in *Mycobacterium tuberculosis*, Science 263 (1994) 227–230.
[4] C.L. Kelley, D.A. Rouse, S.L. Morris, Analysis do *ahpC* gene mutations in isoniazid-reistant clinical isolates of *Mycobacterium tuberculosis*, Antimicrob. Agents Chemother. 41 (1997) 2057–2058.
[5] K. Mdluli, R.A. Slayden, Y. Zhu, S. Ramaswamy, X. Pan, D. Mead, D.D. Crane, J.M. Musser, C.E. Barry, Inhibition of a *Mycobacterium tuberculosis* beta-ketoacyl ACP synthase by isoniazid, Science 280 (1998) 1607–1610.
[6] A.S.G. Lee, A.S.M. Teo, S.Y. Wong, Novel mutations in ndh in isoniazid-resistant *Mycobacterium tuberculosis* isolates, Antimicrob. Agents Chemother. 45 (2001) 2157–2159.
[7] A. van Rie, R. Warren, I. Mshanga, A.M. Jordaan, G.D. van der Spuy, M. Richardson, J. Simpson, R.P. Gie, D.A. Enarson, et al., Analysis for a limited number of gene codons can predict drug resistance of *Mycobacterium tuberculosis* in a high-incidence community, J. Clin. Microbiol. 39 (2001) 636–641.
[8] M.L.R. Rossetti, A.R.M. Valim, M.S.N. Silva, V.S. Rodrigues, Tuberculose resistente: revisão molecular, Rev. Saúde Pública 36 (2002) 525–532.
[9] M.S.N. Silva, S. Senna, M.O. Ribeiro, A.M. Valim, M.A. Telles, A.L. Kritski, G.P. Morlock, R.C. Cooksey, A. Zaha, M.L.R. Rossetti, Mutations in katG, inhA and ahpC genes of brazilian isoniazid-resistant isolates of *Mycobacterium tuberculosis*, J. Clin. Microbiol. 41 (2003) 4471–4474.
[10] E.R. Dalla Costa, M.O. Ribeiro, M.S.N. Silva, L.S. Arnold, D.C. Rostirolla, P.I. Cafrune, R.C. Espinoza, M. Palaci, M. Telles, V. Ritacco, P.N. Suffys, M.L. Lopes, C.L. Campelo, S.S. Miranda, K. Kremer, P.E. Silva Almeida, L.S. Fonseca, J.L. HO, A.L. Kritski, M.L.R. Rossetti, Correlations of mutations in katG, oxyR-ahpC and inhA genes and in vitro susceptibility in *Mycobacterium tuberculosis* clinical strains segregated by spoligotype families from tuberculosis prevalent countries in South America, BMC Microbiol. 9 (2009) 1–11.
[11] M. Viveiros, C. Leandro, L. Amaral, Mycobacterial efflux pumps and chemotherapeutic implications, Int. J. Antimicrob. Agents 22 (2003) 274–278.
[12] A.M. Upton, A. Mushtaq, T.C. Victor, S.L. Sampson, J. Sandy, D.M. Smith, P.D. van Helden, E. Sim, Arylamine N-acetyltransferase of *Mycobacterium tuberculosis* is a polymorphic enzyme and a site of isoniazid metabolism, Mol. Microbiol. 42 (2001) 309–317.
[13] C. Sholto-Douglas-Vernon, J. Sandy, T.C. Victor, E. Sim, P.D. van Helden, Mutational and expression analysis of tbnat and its response to isoniazid, J. Med. Microbiol. 54 (2005) 1189–1197.
[14] J. Sandy, A. Mushtaq, S.J. Holton, P. Schartau, M.E.M. Noble, E. Sim, Investigation of the catalytic triad of arylamine N-acetyltransferases: essential residues required for acetyl transfer to arylamines, Biochem. J. 390 (2005) 115–123.
[15] E. Sim, I. Westwood, E. Fullam, Arylamine N-acetyltransferases, Expert Opin Drug Metab. Toxicol. 3 (2007) 169–184.
[16] E. Fullam, I.M. Westwood, M.C. Anderton, E.D. Lowe, E. Sim, M.E. Noble, Divergence of cofator recognition across evolution: coenzyme A binding in a prokaryotic arylamine N-acetyltransferase, J. Mol. Biol. 375 (2008) 178–191.
[17] E. Sim, M. Payton, M. Noble, R. Minchin, An update on genetic, structural and functional studies of arylamine N-acetyltransferase in eucaryotes and prokaryotes, Hum. Mol. Genet. 9 (2000) 2435–2441.
[18] J. Sandy, A. Mushtaq, A. Kawamura, J. Sinclair, E. Sim, M. Noble, The structure of arylamine N-acetyltranferase from *Mycobacterium smegmatis*–an enzyme which inactivates the anti-tubercular drug, isoniazid, J. Mol. Biol. 318 (2002) 1071–1083.
[19] M. Payton, R. Auty, R. Delgoda, M. Everett, E. Sim, Cloning and characterization of arylamine N-acetyltransferase genes from *Mycobacterium smegmatis* and *Mycobacterium tuberculosis*: increased expression results in isoniazid resistance, J. Bacteriol. 181 (1999) 1343–1347.
[20] P.T. Kent, G.P. Kubica, Public Health Mycobacteriology: A Guide for a Level III Laboratory, Butterworth-Heinemann/Centers for Disease Control, Oxford, UK/Atlanta, GA, USA, 1985.
[21] G. Canetti, W. Fox, A. Khomenko, H.T. Mahler, N.K. Menom, D.A. Mitchison, N. Rist, N.A. Smeley, Advancesin techniques of testing mycobacterial drug sensivity, and the use of sensivity tests in tuberculosis control programmes, Bull. WHO 41 (1969) 21–43.
[22] J.C. Palomino, A. Martin, M. Camacho, H. Guerra, J. Swings, F. Portaels, Resazurin microtiter assay plate: simple and inexpensive meted for detection of drug resistance in *Mycobacterium tuberculosis*, Antimicrob. Agents Chemother. 46 (2002) 2720–2722.
[23] D. van Soolingen, P.E. de Haas, P.W. Hermans, J.D. van Embden, DNA fingerprinting of *Mycobacterium tuberculosis*, Methods Enzymol. 235 (1994) 196–204.
[24] A. Telenti, N. Honoré, C. Bernasconi, J. March, A. Ortega, B. Heym, H.E. Takiff, S.T. Cole, Genotypic assessment of isoniazid and rifampin resistance in *Mycobacterium tuberculosis*: a blind study at reference laboratory level, J. Clin. Microbiol. 35 (1997) 719–723.
[25] T.D. Otto, E.A. Vasconcellos, L.H.F. Gomes, A.S. Moreira, W.M. Degrave, L. Mendonça-Lima, M. Alves-Ferreira, ChromaPipe: a pipeline for analysis, quality control and management for a DNA sequencing facility, Genet. Mol. Res. 7 (2008) 861–871.
[26] J. Kamerbeek, L. Schouls, A. Kolk, M. van Agterveld, D. van Soolingen, S. Kuijper, A. Bunschoten, H. Molhuizen, R. Shaw, M. Goyal, J. van, Embden, Simultaneous detection and strain differentiation of mycobacterium tuberculosis for diagnosis and epidemiology, J. Clin. Microbiol. 35 (1997) 907–914.
[27] N. Eswar, M.A. Marti-Renom, B. Webb, M.S. Madhusudhan, D. Eramian, M. Shen, U. Pieper, A. Sali, Comparative protein structure modeling with modeller, Curr. Protoc. Protein Sci. 50 (2.9.) (2007) 1–31.
[28] A. Sali, T.L. Blundell, Comparative protein modelling by satisfaction of spatial restraints, J. Mol. Biol. 234 (1993) 779–815.

[29] M.Y. Shen, A. Sali, Statistical potential for assessment and prediction of protein structures, Protein Sci. 15 (2006) 2507–2512.
[30] H.L. de Amorim, P.A. Netz, J.A. Guimarães, Thrombin allosteric modulation revisited: a molecular dynamics study, J. Mol. Model. 16 (2010) 725–735.
[31] T. Tonjum, D.B. Welty, E. Jantzen, P.L. Small, Differentiation of *Mycobacterium ulcerans*, *M. marinum*, and *M. haemophilum*: mapping of their relationships to M. tuberculosis by fatty acid profile analysis, DNA-DNA hybridization, and 16S rRNA gene sequence analysis, J. Clin. Microbiol. 36 (1998) 918–925.
[32] E. Fullam, A. Kawamura, H. Wilkinson, A. Abuhammad, I. Westwood, E. Sim, Comparison of the arylamine N-acetyltransferase from *Mycobacterium marinum* and *Mycobacterium tuberculosis*, Protein J. 28 (2009) 281–293.
[33] J. Sandy, S. Holton, E. Fullam, E. Sim, M. Noble, Binding of the anti-tubercular drug isoniazid to the arilamine N-acetyltransferase protein from *Mycobacterium smegmatis*, Protein Sci. 14 (2005) 775–782.
[34] R.A. Laskowski, M.W. MacArthur, D.S. Moss, J.M. Thornton, PROCHECK: a program to check the stereochemical quality of protein structures, J. Appl. Crystallogr. 26 (1993) 283–291.
[35] J.U. Bowie, R. Luthy, D. Eisenberg, A method to identify protein sequences that fold into a known three-dimensional structure, Science 253 (1991) 164–170.
[36] C. Colovos, T.O. Yeates, Verification of protein structures: patterns of nonbonded atomic interactions, Protein Sci. 2 (1993) 1511–1519.
[37] H. Wu, L. Dombrovsky, W. Tempel, F. Martin, P. Loppnau, G.H. Goodfellow, D.M. Grant, A.N. Plotnikov, Structural basis of substrate-binding specificity of human arylamine N-acetyltransferases, J. Biol. Chem. 282 (2007) 30189–30197.
[38] A. Mushtaq, M. Payton, E. Sim, The COOH terminus of arylamine N-acetyltransferase from *Salmonella typhimurium* controls enzymic activity, J. Biol. Chem. 277 (2002) 12175–12181.
[39] H.R. van Doorn, P.E.W. de Haas, K. Kremer, C.M.J. Vandenbroucke-Grauls, M.W. Borgdorff, D. van Soolingen, Public health impact of isoniazid-resistant *Mycobacterium tuberculosis* strains with a mutation at amino-acid position 315 of katG: a decade of experience in The Netherlands, Clin. Microbiol. Infect. 12 (2006) 769–775.
[40] A.L. Sikora, B.A. Frankel, J.S. Blanchard, Kinetic and chemical mechanism of arylamine n-acetyltransferase from *Mycobacterium tuberculosis*, Biochemistry 47 (2008) 10781–10789.
[41] K. Brudey, J.R. Driscoll, L. Rilgouts, W.N. Prodinger, A. Gori, S.A. Al-Hajoi, C. Allix, L. Aristimuno, et al., Mycobacterium tuberculosis complex genetic diversity: mining the fourth international spoligotyping database (SpolDB4) for classification, population genetics and epidemiology, BMC Microbiol. 6 (2006).
[42] R.A. Engh, R. Huber, Accurate bond and angle parameters for X-ray protein structure refinement, Acta Crystallogr. 47 (1991) 392–400.